




Article

# Loss of the R2R3 MYB Transcription Factor RsMYB1 Shapes Anthocyanin Biosynthesis and Accumulation in *Raphanus sativus*

Da-Hye Kim <sup>1,2</sup>, Jundae Lee <sup>3</sup> , JuHee Rhee <sup>2</sup>, Jong-Yeol Lee <sup>2,\*</sup> and Sun-Hyung Lim <sup>1,\*</sup>

<sup>1</sup> Division of Horticultural Biotechnology, School of Biotechnology, Hankyong National University, Anseong 17579, Korea; kimdh143@naver.com

<sup>2</sup> National Institute of Agricultural Sciences, Rural Development Administration, Jeonju 54874, Korea; rheehk@korea.kr

<sup>3</sup> Department of Horticulture, Institute of Agricultural Science & Technology, Jeonbuk National University, Jeonju 54896, Korea; ajfall@jbnu.ac.kr

\* Correspondence: jy0820@korea.kr (J.-Y.L.); limsh2@hknu.ac.kr (S.-H.L.);  
Tel.: +82-63-238-4616 (J.-Y.L.); +82-31-670-5105 (S.-H.L.)

**Abstract:** The red or purple color of radish (*Raphanus sativus* L.) taproots is due to anthocyanins, which have nutritional and aesthetic value, as well as antioxidant properties. Moreover, the varied patterns and levels of anthocyanin accumulation in radish roots make them an interesting system for studying the transcriptional regulation of anthocyanin biosynthesis. The R2R3 MYB transcription factor RsMYB1 is a key positive regulator of anthocyanin biosynthesis in radish. Here, we isolated an allele of *RsMYB1*, named *RsMYB1<sup>Short</sup>*, in radish cultivars with white taproots. The *RsMYB1<sup>Short</sup>* allele carried a 4 bp insertion in the first exon causing a frame-shift mutation of *RsMYB1*, generating a truncated protein with only a partial R2 domain at the N-terminus. Unlike *RsMYB1<sup>Full</sup>*, *RsMYB1<sup>Short</sup>* was localized to the nucleus and the cytoplasm and failed to interact with their cognate partner *RsTT8*. Transient expression of genomic or cDNA sequences for *RsMYB1<sup>Short</sup>* in radish cotyledons failed to induce anthocyanin accumulation, but that for *RsMYB1<sup>Full</sup>* activated it. Additionally, *RsMYB1<sup>Short</sup>* showed the lost ability to induce pigment accumulation and to enhance the transcript level of anthocyanin biosynthetic genes, while *RsMYB1<sup>Full</sup>* promoted both processes when co-expressed with *RsTT8* in tobacco leaves. As the result of the transient assay, co-expressing *RsTT8* and *RsMYB1<sup>Full</sup>*, but not *RsMYB1<sup>Short</sup>*, also enhanced the promoter activity of *RsCHS* and *RsDFR*. We designed a molecular marker for *RsMYB1* genotyping, and revealed that the *RsMYB1<sup>Short</sup>* allele is common in white radish cultivars, underscoring the importance of variation at the *RsMYB1* locus in anthocyanin biosynthesis in the radish taproot. Together, these results indicate that the nonsense mutation of *RsMYB1* generated the truncated protein, *RsMYB1<sup>Short</sup>*, that had the loss of ability to regulate anthocyanin biosynthesis. Our findings highlight that the frame shift mutation of *RsMYB1* plays a key role in anthocyanin biosynthesis in the radish taproot.

**Keywords:** anthocyanin; frameshift mutation; MBW complex; radish; *RsMYB1*



**Citation:** Kim, D.-H.; Lee, J.; Rhee, J.; Lee, J.-Y.; Lim, S.-H. Loss of the R2R3 MYB Transcription Factor *RsMYB1* Shapes Anthocyanin Biosynthesis and Accumulation in *Raphanus sativus*. *Int. J. Mol. Sci.* **2021**, *22*, 10927. <https://doi.org/10.3390/ijms222010927>

Academic Editor: Alessandro Attanzio

Received: 14 September 2021

Accepted: 4 October 2021

Published: 10 October 2021

**Publisher's Note:** MDPI stays neutral with regard to jurisdictional claims in published maps and institutional affiliations.



**Copyright:** © 2021 by the authors. Licensee MDPI, Basel, Switzerland. This article is an open access article distributed under the terms and conditions of the Creative Commons Attribution (CC BY) license (<https://creativecommons.org/licenses/by/4.0/>).

## 1. Introduction

Anthocyanins are flavonoid-derived metabolites with multiple functions, which include attracting pollinators or seed dispersal agents, protecting plants against damage from UV radiation, and contributing to cold and drought stress responses [1,2]. In addition, anthocyanins have strong antioxidant activity and have attracted widespread interest due to their health benefits in preventing chronic human diseases, certain cancers, and cardiovascular diseases [3–5].

The anthocyanin biosynthetic pathway has been well characterized and genes encoding the relevant enzymes and transcriptional regulators have been identified in many plant species [6]. Anthocyanin biosynthesis is transcriptionally regulated by R2R3 MYB transcription factors (TFs), basic helix-loop-helix (bHLH) TFs, and WD40 repeat proteins,

which interact to form MYB–bHLH–WD40 (MBW) complexes [7,8]. Among these regulators, the MYB proteins contain two conserved imperfect repeats (named R2 and R3) in their N terminus and a variable region in the C terminus, which is responsible for their regulatory activity [9,10]. The bHLH factors form transcriptional complexes at the promoters of anthocyanin biosynthetic genes by interacting with the R3 region of their R2R3 MYB partners [11,12]. Within the complex, the WD40 partners act as a docking platform and stabilize the interaction between the MYB and bHLH TFs, rather than exerting a direct regulatory function [7,13].

Different MYB genes are expressed at different levels in different tissues as a function of developmental stage and environmental conditions; the set of MYB TFs in a specific tissue conditions the differential accumulation of flavonoids in that tissue by affecting the target gene specificity of the MBW complex, and thus the expression of specific anthocyanin biosynthesis genes [14,15]. Therefore, the correct distribution of anthocyanins in plant tissues requires accurate spatial and temporal regulation of the flavonoid biosynthetic pathway and reflects tissue-specific combinations of transcription factors.

In the MBW complex, the R2R3 MYB determines the spatio-temporal pattern of anthocyanin production and accumulation [16,17]. Several studies have demonstrated that loss of R2R3 MYB function is accompanied by defects in anthocyanin accumulation [18,19]. For example, mutations in *FvMYB10-1* from diploid strawberry (*Fragaria vesca*) and *CgRuby1<sup>short</sup>* from citrus (*Citrus grandis*) impair the function of the encoded R2R3 MYB TFs in activating anthocyanin biosynthesis [18,19]. The insertions of long terminal repeat (LTR) transposable elements in an exon of octoploid strawberry (*F. × ananassa*) *FaMYB10-1* or an intron of Chinese cabbage (*Brassica rapa* L.) *BrMYB2* are similarly associated with the lack of pigmentation of these species [19,20]. Likewise, a mutation affecting the splicing of tomato (*Solanum lycopersicum*) *ANTHOCYANIN 2-like* (*SIAN2-like*) transcripts results in a complete loss of anthocyanin accumulation [21].

In some cases, the *cis*-regulatory element recognized by the R2R3 MYB may also be present in the promoter region of its encoding gene, thus forming an auto-regulatory loop. For example, comparison of the proximal *MdMYB10* promoter regions between white-fleshed and green-foliaged apples (*Malus domestica*) revealed a single copy of a 23 bp sequence, whereas red-fleshed and red-foliaged apples contained six copies of an almost identical sequence as a minisatellite-like structure that was critical to the modulation of *MdMYB10* transactivation [22]. Indeed, mutating or deleting this repeat sequence in the *MdMYB10* promoter caused a strong reduction in transactivation by preventing autoregulation. In addition, blood orange (*Citrus × sinensis* ‘Blood orange’) gained its intense coloration from an LTR-retrotransposon insertion in the promoter of a gene encoding an R2R3 MYB TF, leading to the transcriptional activation of *CgRuby1* [23]. Similarly, purple-fruited peppers (*Capsicum annuum*) harbor a non-LTR retrotransposon insertion in the *CaAN2* promoter that is sufficient to activate the transcription of *CaAN2* [24]. The red color displayed by red-fleshed strawberries is also strongly associated with enhanced expression of *FaMYB10-2* due to an insertion of a CACTA-like transposon (*FaEnSpm-2*) in its promoter [19].

Radish (*Raphanus sativus* L.) is a member of the Brassicaceae family, and an economically important taproot vegetable crop grown globally. Radish taproots vary in color from white to red, purple-pink, or green, or even display two colors, depending on the accumulation and distribution of anthocyanins and chlorophyll [25,26]. Therefore, radish provides an interesting system for the study of the regulation of anthocyanin biosynthesis. Moreover, genes involved in anthocyanin biosynthesis have been cloned in radish. For example, the radish *RsMYB1* and *TRANSPARENT TESTA 8* (*RsTT8*) genes encode an R2R3 MYB and a bHLH TF, respectively [12,27]. Transient co-infiltration of constructs expressing these two genes in tobacco (*Nicotiana tabacum*) leaves confirmed their contribution to anthocyanin accumulation and the activation of anthocyanin biosynthetic genes, including *CHALCONE SYNTHASE* (*RsCHS*) and *DIHYDROFLAVONOL 4-REDUCTASE* (*RsDFR*) [12].

The transcriptional and epigenetic regulation of the key activator of anthocyanin biosynthesis *RsMYB1* (also called *RsMYB90*) orchestrates anthocyanin biosynthesis in radish taproots [27–29]. For example, hypermethylation of the *RsMYB1* promoter results in low *RsMYB1* transcription rates and white-fleshed taproots due to the lack of anthocyanin biosynthesis [30]. In addition, a retrotransposon insertion into a gene encoding a flavonoid 3'-hydroxylase (F3'H) in radishes with purple taproots causes a red color due to pelargonidin-based anthocyanin accumulation [31].

Here, we identify a novel allele of *RsMYB1* (*RsMYB1<sup>Short</sup>*) and examine *RsMYB1* function in determining anthocyanin accumulation in radish taproots. The variants *RsMYB1<sup>Full</sup>* from red/purple radish and *RsMYB1<sup>Short</sup>* from white radish confer their characteristic taproot colors by exerting opposite effects on the regulation of anthocyanin biosynthesis. Based on *RsMYB1* variants in various radish cultivars, we also developed a molecular marker for the marker-assisted selection and prediction of radish lines with red/purple taproots. This study thus helps unravel the regulatory mechanisms underlying anthocyanin biosynthesis in radish taproots.

## 2. Results

### 2.1. Anthocyanin Accumulation Determines the Red and Purple Color of Radish Roots

We grew plants from all radish cultivars in a growth room and in the field to confirm their phenotypes after 8 weeks of growth. The three white cultivars W1, W2, and W3 showed no evidence of red color in their roots, whereas the skin of R1 cultivar taproots, as well as the root skin and root flesh of the R2 cultivar, had a clearly visible red color (Figure 1A). Interestingly, the R3 cultivar had purple root skin and flesh.

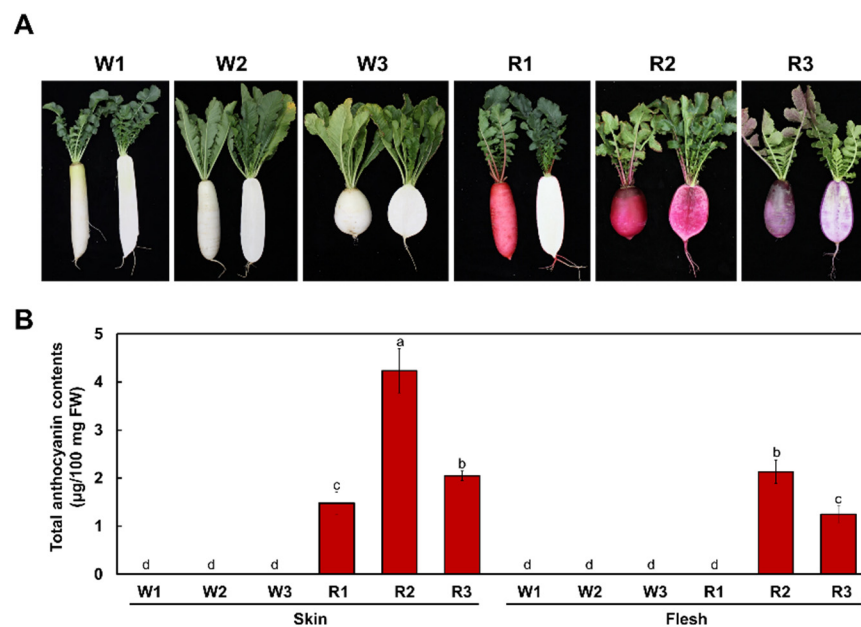


**Figure 1.** Phenotypes and anthocyanin contents of the six radish cultivars used in this study. (A) Representative photographs of white- and red-taproot radishes at the mature stage, with whole taproots on the left and taproots sectioned to show flesh color on the right of each image. (B) Anthocyanin levels in white and red taproot radishes. Results are mean values  $\pm$  SD from three independent biological replicates. Different letters above the bars indicate significantly different values ( $p < 0.0001$ , one-way ANOVA followed by Duncan's multiple range test).

To quantify the pigment contents of root skins and flesh, we extracted anthocyanins from these tissues and measured their absorbance at 530 nm and 657 nm (Figure 1B). In agreement with the visible phenotypes above, we detected no anthocyanin accumulation in the root skins or flesh of the three white cultivars W1, W2, and W3. However, we measured

high levels of anthocyanins in the root skin, but not in the flesh, of the R1 cultivar. Both the R2 and R3 cultivars accumulated anthocyanins in their root skins and flesh, with higher levels in the skin. Therefore, these results indicate that the pigmentation phenotype of radish taproots was determined by anthocyanin accumulation.

## 2.2. Anthocyanin Biosynthetic Genes Are Highly Expressed in Red and Purple Radish Taproots

We next performed RT-qPCR on three previously identified regulators of anthocyanin biosynthesis, *RsMYB1*, *RsTT8*, and *TRANSPARENT TESTA GLABRA 1* (*RsTTG1*), in the root skin and flesh of the six radish cultivars. *RsMYB1* and *RsTT8* were highly expressed in the root skin of all red and purple cultivars, and their expression reflected the extent of pigment accumulation in these tissues (Figure 2A). In addition, *RsMYB1* and *RsTT8* were more highly expressed in the root skin than in the root flesh of colored cultivars. By contrast, and as previously reported, *RsTTG1* was expressed at similar levels in all tissues independently of anthocyanin accumulation. These results indicate that simultaneous expression of *RsMYB1* and *RsTT8* correlated with anthocyanin accumulation. Indeed, anthocyanin biosynthetic genes were generally expressed to much higher levels in tissues accumulating anthocyanins than in tissues from white radish cultivars (Figure 2B). The general phenylpropanoid biosynthetic gene, *PHENYLALANINE AMMONIA-LYASE* (*RsPAL*), was equally expressed between red and white cultivars. However, early biosynthetic genes (EBGs), including *RsCHS*, *CHALCONE ISOMERASE* (*RsCHI*), and *FLAVANONE 3-HYDROXYLASE* (*RsF3H*), were highly upregulated in the red and purple cultivars, which also show high expression of *RsMYB1* and *RsTT8*. Likewise, the transcript levels of the late biosynthetic genes (LBGs) *RsDFR* and *ANTHOCYANIDIN REDUCTASE* (*RsANS*) were high in the root skins and root flesh of the red and purple cultivars, in agreement with the expression pattern of *RsMYB1* and *RsTT8*. Taken together, these results confirm that anthocyanin accumulation reflected the expression levels of flavonoid biosynthetic genes across the different cultivars, and that this occurred in tissues co-expressing *RsMYB1* and *RsTT8*.

## 2.3. White Taproot Radish Cultivars Harbor a Variant *RsMYB1* Allele

To investigate the mechanism underlying the variation in taproot color, we compared the coding regions of *RsMYB1* and *RsTT8* from white (W1) and red (R1) radish cultivars. *RsMYB1* from the red cultivar exhibited a 93.0% sequence identity to the previously reported *RsMYB1* allele from the purple radish cultivar 'Bordeaux', due to the presence of an insertion/deletion (InDel) polymorphism in an intron and several single-nucleotide polymorphisms (SNPs) in both exons and introns (Supplementary Figure S1). The *RsMYB1* coding sequence from red radish (R1) was 747 bp in length and encoded a predicted protein of 248 amino acids, which we designated *RsMYB1*<sup>Full</sup> (Figure 3A). Likewise, the sequence identity between *RsMYB1* from the white and Bordeaux cultivars was 94.5%, owing to an InDel in an intron and several SNPs in exons and introns. Notably, *RsMYB1* from the white radish cultivar W1 contained a 4 bp (AATT) insertion in the first exon, resulting in the frameshift mutation and early stop codon after five amino acids from this mutation point (Figure 3B). The corresponding protein retained only the 41-amino-acid N-terminal part of *RsMYB1*<sup>Full</sup> that lacked the majority of the downstream residues of the R2 domain and was designated as *RsMYB1*<sup>Short</sup>.

Sequence alignments between anthocyanin-promoting R2R3 MYB TFs belonging to the phylogenetic subgroup 5 (SG5) and subgroup 6 (SG6) from various plants indicated that *RsMYB1*<sup>Full</sup> and *RsMYB1*<sup>Short</sup> cluster with the SG6 clade (Supplementary Figure S2). In addition, this alignment showed that *RsMYB1*<sup>Full</sup> has a typical R2R3 domain with a conserved ANDV motif and a domain through which such R2R3 TFs interact with bHLH TFs ([D/E]Lx2[R/K]x3Lx6Lx3R) in its N terminus, as well as the common SG6 (KPRPR[S/T]F) motif in its C terminus. In contrast, *RsMYB1*<sup>Short</sup> had the only partial R2 domain and was largely truncated in the subsequent region, harboring the R3 domain and activation motif at the C terminus.

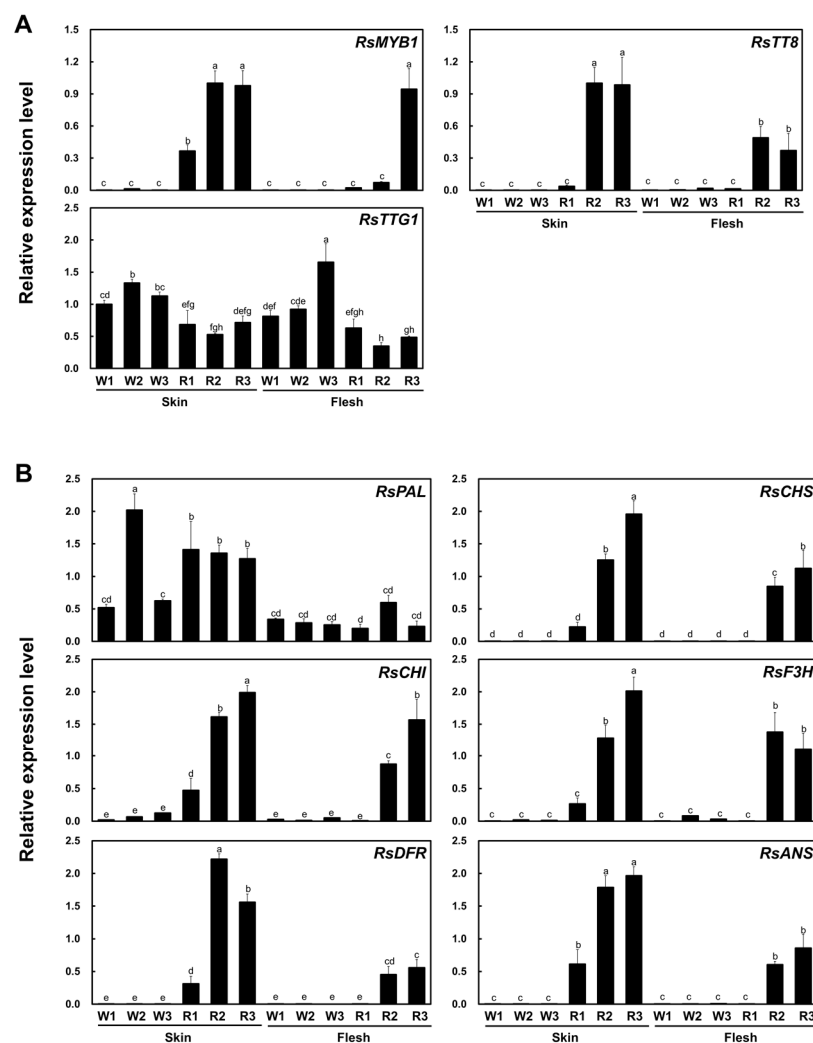


**Figure 2.** Relative transcript levels of anthocyanin biosynthetic and regulatory genes in the six radish cultivars. (A) Anthocyanin biosynthetic regulators. (B) Anthocyanin biosynthetic genes. *RsRPII* was used as a reference gene for evaluating the target gene expression. Results are mean values  $\pm$  SD from three independent biological replicates. Different letters above the bars indicate significantly different values ( $p < 0.05$ , two-way ANOVA followed by Duncan's multiple range test).

#### 2.4. Subcellular Localization Analysis of *RsMYB1<sup>Short</sup>*, *RsMYB1<sup>Full</sup>*, and *RsTT8*

For assessment of the subcellular distribution of *RsMYB1<sup>Short</sup>* and *RsMYB1<sup>Full</sup>*, we transiently transfected *Arabidopsis* mesophyll protoplasts with constructs expressing fusions between the green fluorescent protein (GFP) and *RsMYB1<sup>Short</sup>*, *RsMYB1<sup>Full</sup>*, or *RsTT8*, together with a nuclear localization marker, consisting of the red fluorescent protein (RFP) with the nuclear localization signal (NLS) of the SV40 large T antigen, as a positive control (Figure 4A). We detected strong GFP fluorescence from the nuclei of all protoplasts transfected with the *RsMYB1<sup>Full</sup>-GFP* and *RsTT8-GFP* constructs that co-localized with RFP fluorescence (Figure 4B). However, green fluorescence from *RsMYB1<sup>Short</sup>-GFP* was distributed throughout the cell, including the nucleus and the cytoplasm. Therefore, these results indicate that the frame shift of *RsMYB1* can lead to its abnormal subcellular distribution.

#### 2.5. Frame Shift of *RsMYB1* Affects Its Interaction with *RsTT8*

As shown in Figure 1, *RsMYB1* and *RsTT8* together regulate anthocyanin biosynthetic gene expression in skin and flesh of radish taproot. To examine the interaction between *RsMYB1* and *RsTT8*, we constructed yeast two-hybrid constructs by placing full-length *RsMYB1<sup>Short</sup>* and full-length and partially truncated *RsMYB1<sup>Full</sup>* in-frame with the sequence



encoding the GAL4 activation domain (GAL4-AD) from the pGADT7 vector (Figure 5A). We also generated a set of constructs in the pGBKT7 vector, placing full-length and truncated *RsTT8* in-frame with the sequence coding for the GAL4 DNA-binding domain (BD). We co-transformed appropriate pairs of AD and BD constructs into the yeast strain MaV203 and tested their interaction on stringent selective medium containing 10 mM 3-AT, a competitive inhibitor of the yeast HIS3 enzyme. These assays showed that *RsMYB1*<sup>Full</sup> can interact with *RsTT8*, but *RsMYB1*<sup>Short</sup> cannot. Indeed, we determined that *RsTT8* interacts strongly with partially truncated *RsMYB1*<sup>Full</sup>N2, and *RsMYB1*<sup>Full</sup>N3 as well as *RsMYB1*<sup>Full</sup>L, but not with *RsMYB1*<sup>Full</sup>N1, which only harbored the R2 domain (Figure 5B). Notably, *RsTT8M* and *RsTT8N*, which contained the common MYB interaction region (MIR), interacted with *RsMYB1*<sup>Full</sup>N2, and *RsMYB1*<sup>Full</sup>N3, but not with *RsMYB1*<sup>Full</sup>N1 and *RsMYB1*<sup>Short</sup>. Taken together, these results indicate that the interaction between *RsMYB1* and *RsTT8* may be mediated by an intact R3 domain from *RsMYB1* and the MIR of *RsTT8*, but does not require the bHLH domain of *RsTT8*.

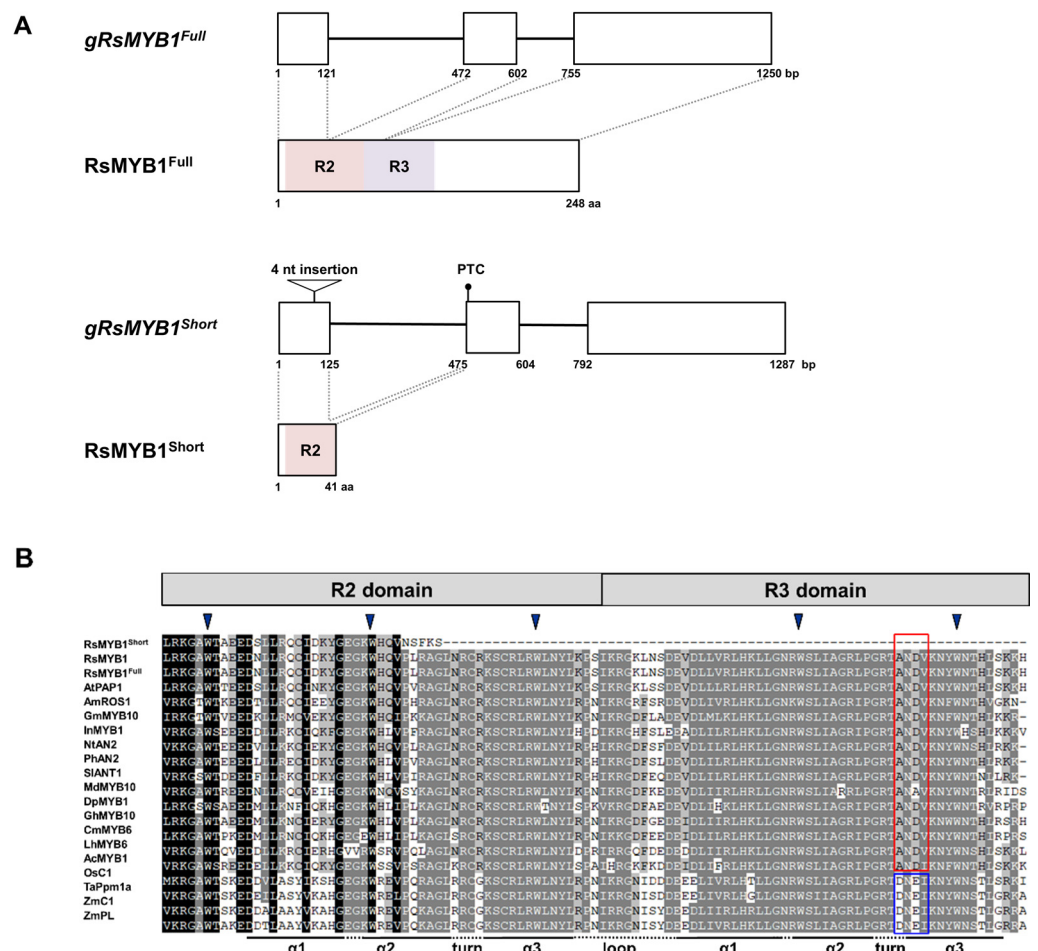


**Figure 3.** Genomic structure of *RsMYB1* alleles and phylogenetic tree of *RsMYB1* proteins from red and white radish cultivars and R2R3 MYB proteins from other plants. (A) Schematic diagram of the genomic structure of *RsMYB1*. The predicted protein encoded by each mature mRNA is indicated below with their functional domains. White boxes, exons; black lines, introns. The 4 bp insertion site in *RsMYB1*<sup>Short</sup> is indicated by a triangle. Premature termination codon (PTC) is indicated by a circle. (B) Multiple protein sequence alignment of the R2 and R3 domains across R2R3 MYB proteins from other plants. The conserved residues of the DNEI and ANDV motifs are shown in the red and blue boxes, respectively. Inverted blue triangles indicate the conserved residues forming the inner hydrophobic core of the R2 and R3 domains.

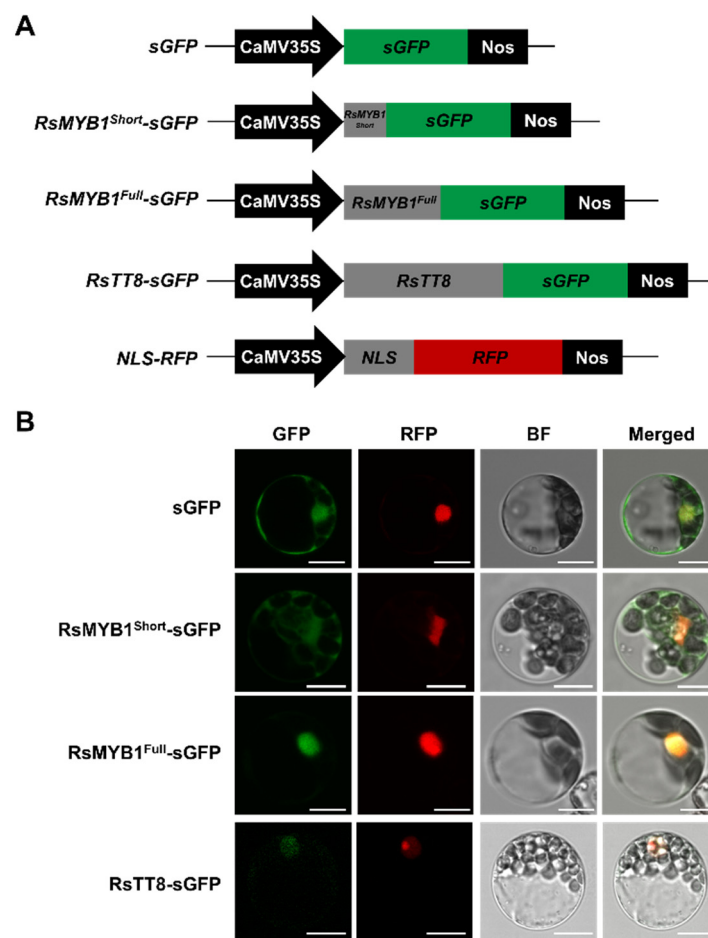


**Figure 4.** Subcellular localization of RsMYB1<sup>Short</sup>, RsMYB1<sup>Full</sup>, and RsTT8 in Arabidopsis leaf protoplasts. **(A)** Schematic diagrams of the constructs: CaMV35S, cauliflower mosaic virus 35S promoter; sGFP, soluble green fluorescent protein (GFP) gene; RsMYB1<sup>Short</sup>-sGFP, RsMYB1<sup>Short</sup> fused to sGFP; RsMYB1<sup>Full</sup>-sGFP, RsMYB1<sup>Full</sup> fused to sGFP; RsTT8-sGFP, RsTT8 fused to sGFP; NLS-RFP, nuclear localization signal fused to the red fluorescent protein (RFP) gene; Nos, nopaline synthase terminator. **(B)** RsMYB1<sup>Short</sup>, RsMYB1<sup>Full</sup>, and RsTT8 localize to the nucleus in Arabidopsis protoplasts. Data are representative of protoplasts accumulating each fusion protein 16 h after transfection. Scale bars = 10  $\mu$ m.

## 2.6. RsMYB1<sup>Short</sup> Is a Loss of Function Allele for Anthocyanin Biosynthesis

Given that RsMYB1<sup>Short</sup> showed an abnormal subcellular distribution and deficient interacting ability with cognate RsTT8, we suspected that RsMYB1<sup>Short</sup> might be lacking in transactivating its downstream targets. To test this hypothesis, we evaluated the function of RsMYB1<sup>Short</sup> and RsMYB1<sup>Full</sup> on anthocyanin biosynthesis via transient assay in radish cotyledons. The transient overexpression of the full length of the genomic sequence or the cDNA of RsMYB1<sup>Full</sup> induced visible pigment accumulation in radish cotyledons, showing that this protein activated anthocyanin biosynthesis. By contrast, neither genomic nor cDNA of RsMYB1<sup>Short</sup> activated anthocyanin biosynthesis, indicating that RsMYB1<sup>Short</sup> was non-functional (Figure 6). These results thus suggest that the 4 bp insertion in RsMYB1<sup>Short</sup> was responsible for a dysfunctional protein that lost the RsMYB1 function.

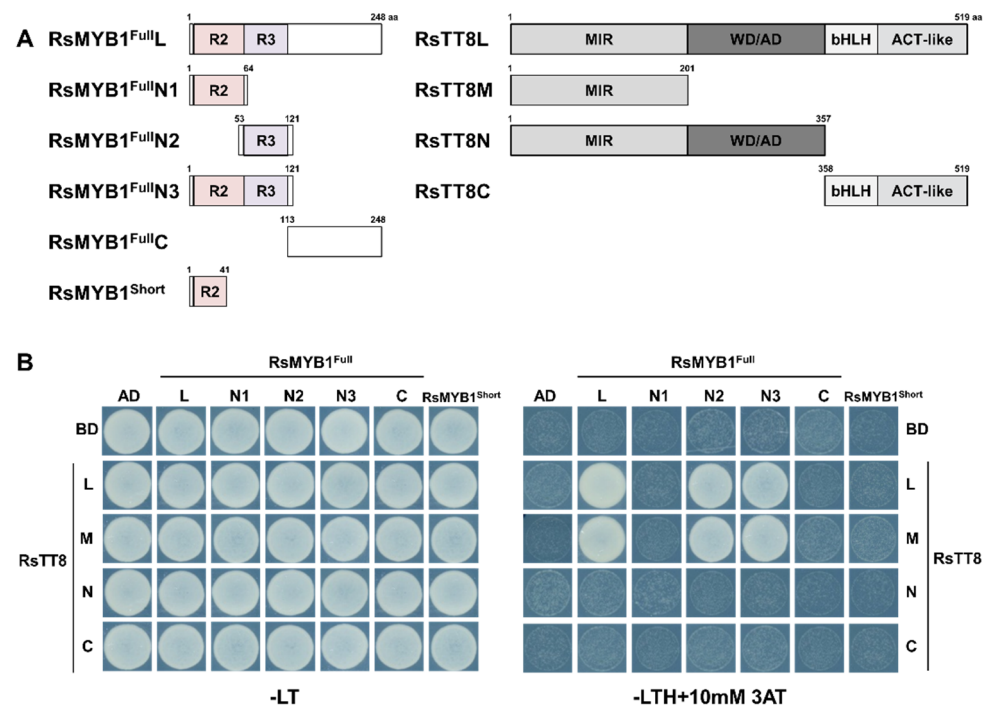


**Figure 5.** Physical interactions among *RsMYB1<sup>Full</sup>*, *RsMYB1<sup>Short</sup>*, and *RsTT8*. (A) Schematic diagrams of the constructs used in the Y2H assay. The amino acid positions of the fragments are shown. (B) Protein–protein interactions among *RsMYB1<sup>Full</sup>*, *RsMYB1<sup>Short</sup>*, and *RsTT8*, as revealed by Y2H analysis. SD/–LT, synthetic defined medium lacking Leu and Trp; SD/–LTH+3AT, SD medium lacking Leu, Trp, and His but containing 10 mM 3-amino-1,2,4-triazole (AT). AD and BD indicate the GAL4 activation domain and binding domain, respectively.

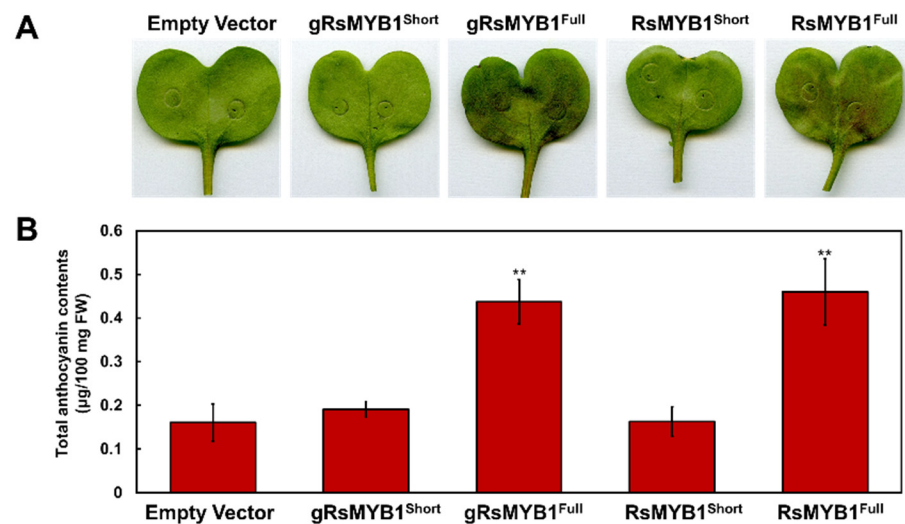


**Figure 6.** Functional analysis of *RsMYB1<sup>Short</sup>* and *RsMYB1<sup>Full</sup>* for anthocyanin biosynthesis. (A) Transient *Agrobacterium*-mediated infiltration assay of constructs expressing *RsMYB1* in radish cotyledons. (B) Anthocyanin contents in transiently infiltrated radish cotyledons shown in A. Results are mean values  $\pm$  SD from three independent biological replicates. \*\*  $p < 0.01$ , as determined by Student's paired  $t$ -test relative to the empty vector.

To obtain an independent confirmation of the respective functions of *RsMYB1<sup>Full</sup>* and *RsMYB1<sup>Short</sup>* in anthocyanin biosynthesis, we repeated the transient infiltration assay in tobacco leaves. Similar to the results with radish cotyledons, we detected the visible accumulation of pigments only with constructs expressing *RsMYB1<sup>Full</sup>* and *RsTT8*, as



cDNAs or a genomic sequence (Figure 7A,B). However, the overexpression of *RsMYB1<sup>Short</sup>* did not induce pigment accumulation, with or without the co-expression of *RsTT8*. The extraction of anthocyanins from each leaf section corroborated the visible phenotypes (Figure 7C).

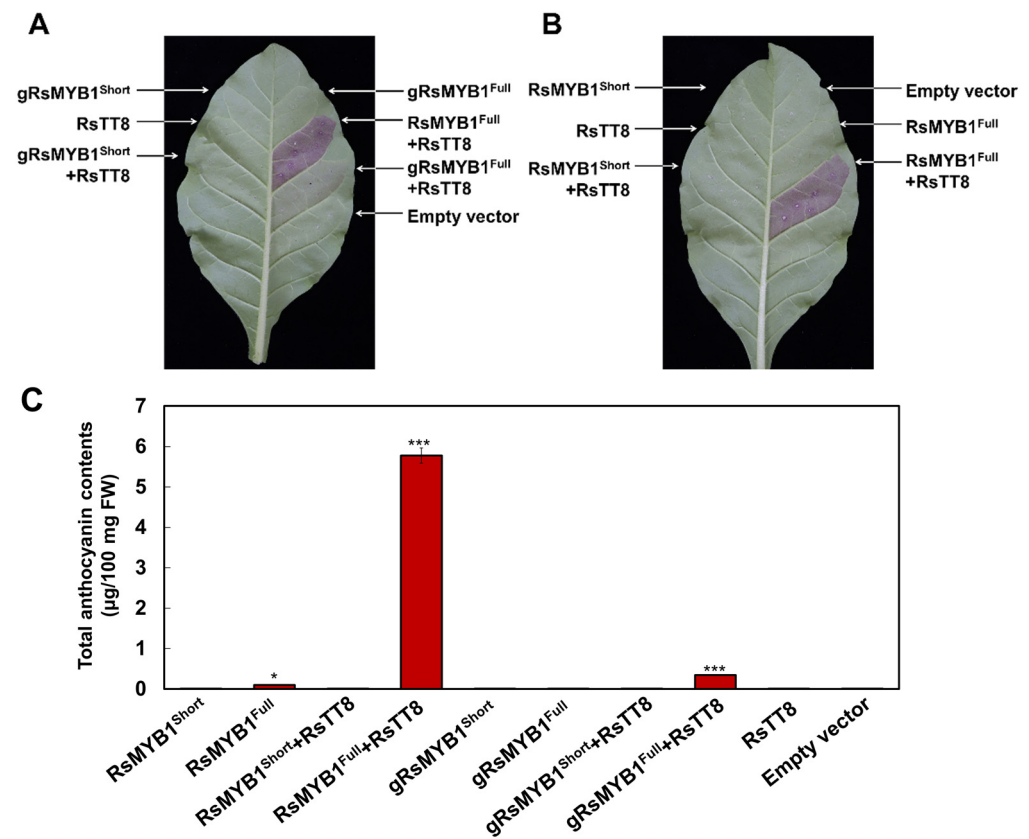


**Figure 7.** Visible phenotypes and anthocyanin contents of tobacco leaves transiently expressing *RsMYB1* constructs. (A) Tobacco leaves transiently infiltrated with constructs carrying the genomic sequence from *RsMYB1<sup>Short</sup>* or *RsMYB1<sup>Full</sup>* alone or together with *RsTT8*. (B) Tobacco leaves transiently infiltrated with constructs carrying the cDNAs from *RsMYB1<sup>Short</sup>* or *RsMYB1<sup>Full</sup>* alone or together with *RsTT8*. (C) Anthocyanin contents of the leaf sectors shown in A and B. Results are mean values  $\pm$  SD from three independent biological replicates. \*  $p < 0.05$ ; and \*\*\*  $p < 0.001$ , as determined by Student's paired *t*-test relative to the empty vector.

To explore the relationship between the expression of anthocyanin biosynthesis genes and anthocyanin contents, we measured the transcript levels of ten structural genes involved in anthocyanin biosynthesis in infiltrated tobacco leaves (Figure 8). We focused on the upstream genes *NtPAL* and *4-COUMARATE:COA LIGASE (Nt4CL)*, the EBGs *NtCHS*, *NtCHI*, *NtF3H*, *NtF3'H*, and *FLAVONOL SYNTHASE (NtFLS)*, and the LBGs *NtDFR*, *NtANS*, and *UDP-GLUCOSE: FLAVONOID 3-O-GLUCOSYLTRANSFERASE (NtUFGT)*. The transient overexpression of *RsMYB1<sup>Short</sup>* alone did not induce the transcription of any anthocyanin biosynthetic genes, as transcript levels were comparable to those of the control transfected with empty vector and to those following *RsTT8* transient overexpression. By contrast, transient expression of *RsMYB1<sup>Full</sup>* alone or in combination with *RsTT8* activated the transcription of anthocyanin biosynthetic genes, with the exception of *NtPAL*, *Nt4CL*, and *NtFLS*, which showed high transcript levels in all samples, including the control transfected with empty vector. We concluded from these results that the *RsMYB1<sup>Full</sup>* allele, but not the *RsMYB1<sup>Short</sup>* allele, was correctly transcribed and translated into a functional protein, even in a heterologous system such as tobacco. These results verify that the 4 bp insertion specific to *RsMYB1<sup>Short</sup>* led to a non-functional allele in both radish and tobacco.

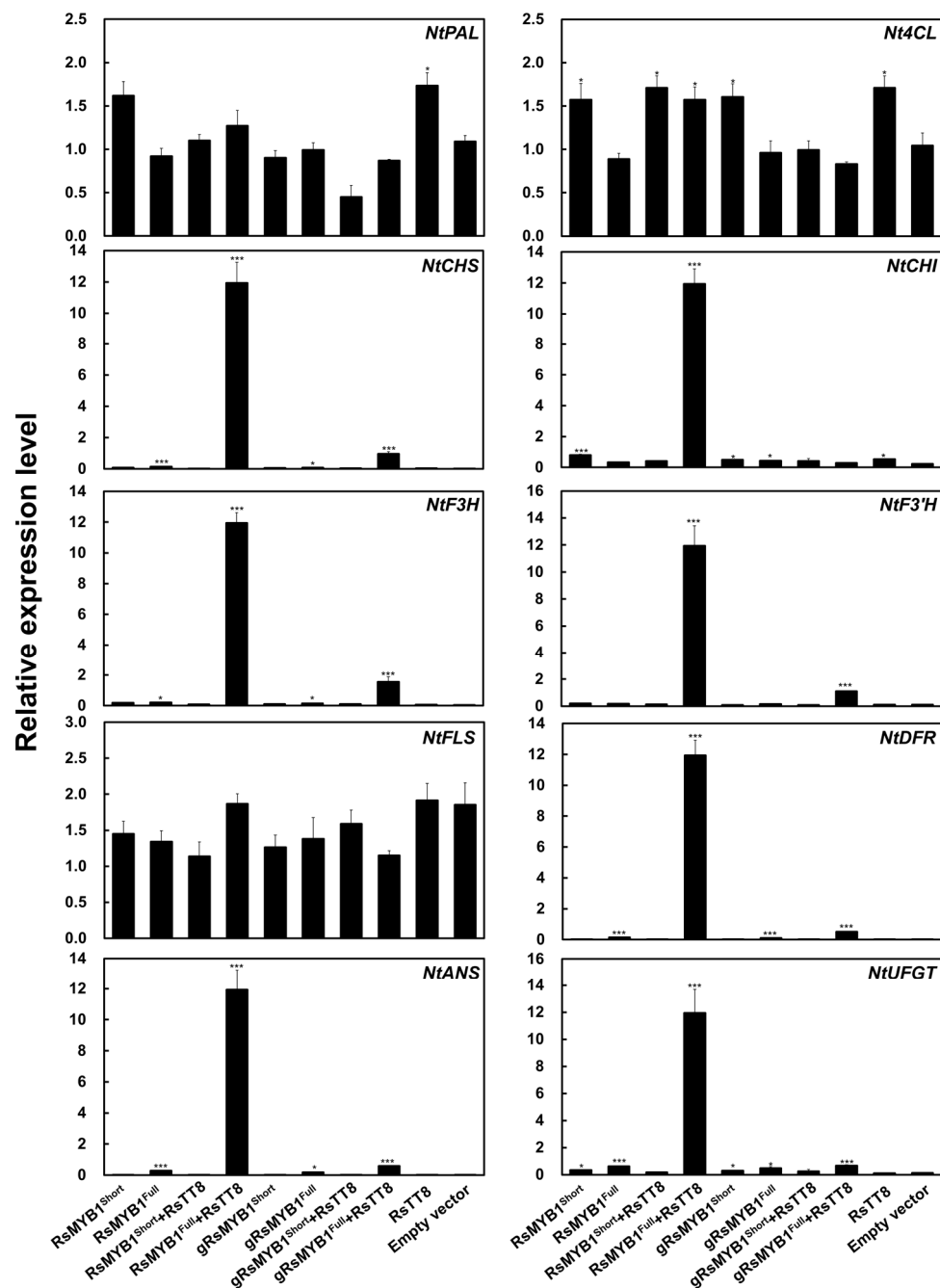


**Figure 8.** Relative transcript levels of anthocyanin biosynthetic genes in tobacco leaves transiently expressing *RsMYB1* constructs. *NtGAPDH* was used as a reference gene. Results are mean values  $\pm$  SD from three independent biological replicates. \*  $p < 0.05$ ; \*\*\*  $p < 0.001$ , as determined by Student's paired *t*-test relative to the empty vector.

### 2.7. *RsMYB1*<sup>Short</sup> Cannot Transactivate the *RsCHS* and *RsDFR* Promoters

Previous studies reported that *RsMYB1*-mediated activation of the *RsCHS* and *RsDFR* promoters was enhanced by the *RsTT8* [12]. To directly link *RsMYB1*<sup>Short</sup> and *RsMYB1*<sup>Full</sup> to anthocyanin biosynthesis, we performed a transient promoter activation assay in tobacco leaves by co-infiltrating effector constructs overexpressing the coding sequences of *RsMYB1*<sup>Short</sup>, *RsMYB1*<sup>Full</sup>, or *RsTT8* with reporter constructs in which the  $\beta$ -*GLUCURONIDASE* (*GUS*) reporter gene was driven by the *RsCHS* or *RsDFR* promoter. As previously reported [12], overexpression of *RsMYB1*<sup>Full</sup> was sufficient to transactivate the *RsDFR* promoter, but not the *RsCHS* promoter (Figure 9). However, both the *RsCHS*

and *RsDFR* promoters showed strong induction when the *RsMYB1<sup>Full</sup>* and *RsTT8* effector constructs were co-infiltrated. Notably, the overexpression of *RsMYB1<sup>Short</sup>* alone or with *RsTT8* failed to transactivate the *RsCHS* and *RsDFR* promoters. The Y2H assay demonstrated that *RsMYB1<sup>Short</sup>* may exist in the small part of the R2 domain due to the frameshift mutation, resulting in the loss of the ability to interact with *RsTT8* (Figure 5). These results indicate that the intactness of *RsMYB1* plays a crucial role in anthocyanin biosynthesis, via interacting with its bHLH partner *RsTT8*.

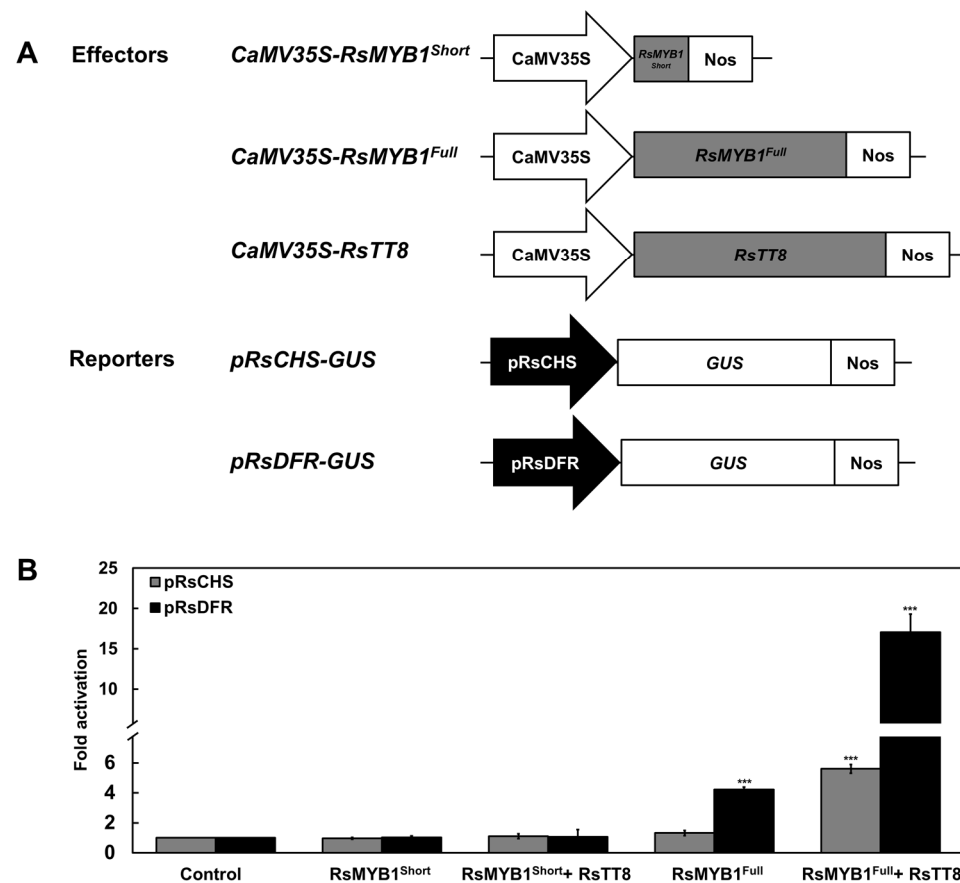


**Figure 9.** Transcriptional activation assay of the *RsCHS* and *RsDFR* promoters by *RsMYB1<sup>Full</sup>*, *RsMYB1<sup>Short</sup>*, and *RsTT8*. (A) Schematic diagrams of effector and reporter constructs used in the transcriptional activation assay. The effector construct harbors the coding sequences of *RsMYB1<sup>Full</sup>*, *RsMYB1<sup>Short</sup>*, and *RsTT8*, respectively, driven by the 35S promoter and NOS terminator. The reporter constructs carry the *RsCHS* and *RsDFR* promoters driving *GUS* expression. (B) Regulatory consequences of the transient expression of *RsMYB1<sup>Short</sup>*, *RsMYB1<sup>Full</sup>*, and *RsTT8* on *RsCHS* and *RsDFR* promoter activity. Results are mean values  $\pm$  SD from three independent biological replicates. \*\*\*  $p < 0.001$ , as determined by Student's paired *t*-test relative to the control.

### 2.8. Additional Unknown Factors Influence Anthocyanin Biosynthesis in Radish Taproots

With the goal of developing a molecular marker to discriminate between the *RsMYB1<sup>Short</sup>* and *RsMYB1<sup>Full</sup>* alleles and assess the association between the genotype at *RsMYB1* and taproot color, we analyzed 20 radish cultivars for variation at *RsMYB1*. Accordingly, we developed a cleaved amplified polymorphic sequence (CAPS) marker based on the variation in the first exon of *RsMYB1* (Supplementary Figure S1). We then genotyped 20 radish cultivars with different taproot colors using this new marker; as positive controls, we included PCR samples using plasmids containing genomic sequences from *RsMYB1<sup>Short</sup>* and *RsMYB1<sup>Full</sup>* as templates. Undigested PCR amplicons for *RsMYB1<sup>Full</sup>* and *RsMYB1<sup>Short</sup>* were 216 bp and 220 bp in size, respectively, but the 4 bp insertion specific to *RsMYB1<sup>Short</sup>* introduced a restriction site for the enzyme *MluCI* (Figure 10). Digested PCR products

for the *RsMYB1<sup>Full</sup>* allele yielded two fragments (185 and 31 bp), while digested PCR products derived from the *RsMYB1<sup>Short</sup>* allele yielded three fragments (145, 44, and 31 bp), demonstrating the validity of the CAPS marker. Importantly, all radish cultivars with red taproots shared the *RsMYB1<sup>Full</sup>* allele, whereas cultivars with white taproots were either homozygous for the *RsMYB1<sup>Short</sup>* (four cultivars) or the *RsMYB1<sup>Full</sup>* allele (three cultivars), or heterozygous for *RsMYB1<sup>Short</sup>* and *RsMYB1<sup>Full</sup>* (three cultivars). These results indicate that the genotype at *RsMYB1* contributes to radish taproot color development. However, since the *RsMYB1* gene alone cannot distinguish radish taproot color, further studies on additional candidate genes for marker development are needed.

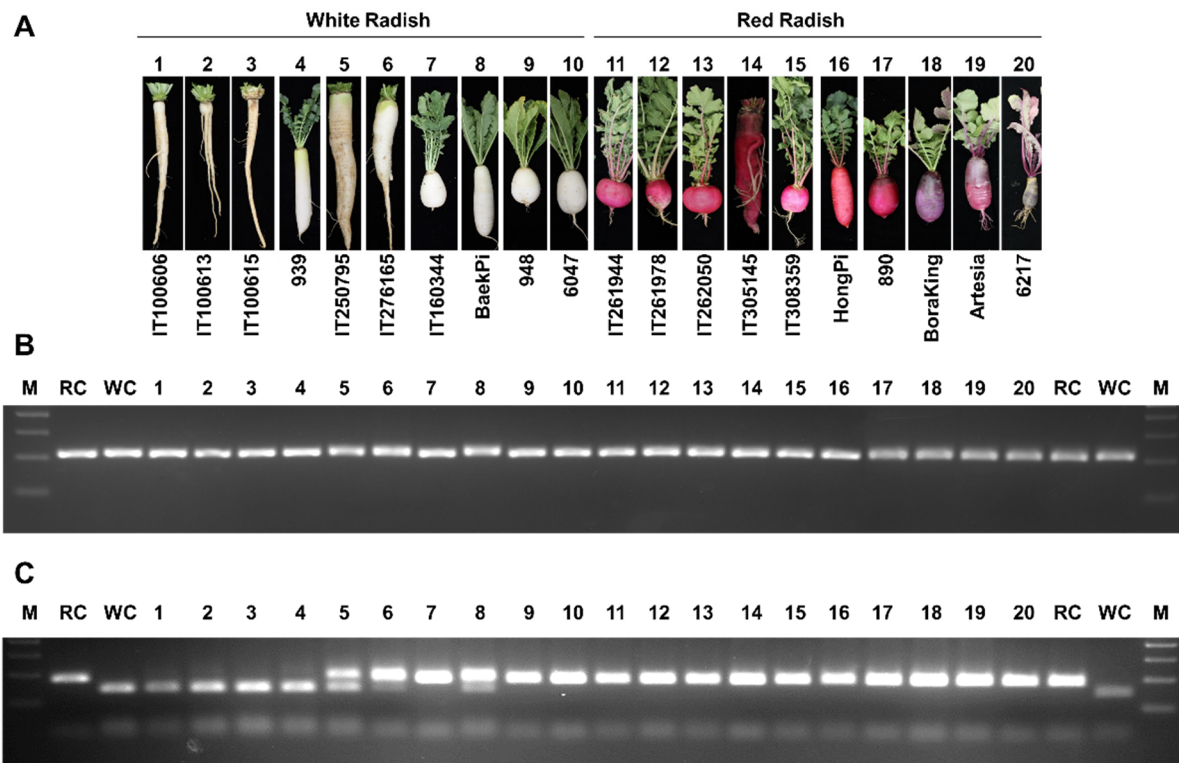


**Figure 10.** Sequence variation at *RsMYB1* predicts taproot color across 20 radish cultivars. (A) Representative photographs of radish taproots showing the different colors of the indicated cultivars. (B) Gel electrophoresis of amplified fragments of the *RsMYB1* gene. (C) Genotyping results of the 20 radish cultivars with the CAPS marker for *RsMYB1*. FC and SC are PCR amplicons from plasmids harboring *RsMYB1<sup>Short</sup>* or *RsMYB1<sup>Full</sup>*, respectively, as positive controls. M: 100 bp DNA size marker.

### 3. Discussion

We discovered that a 4 bp insertion of the anthocyanin biosynthesis regulator gene *RsMYB1* abolishes anthocyanin accumulation in radish. This insight into the regulatory mechanisms behind anthocyanin biosynthesis and its spatio-temporal control has significant implications for the development of designer plant and fruit varieties engineered to have higher or lower levels of anthocyanins through conventional or advanced breeding methods.

#### 3.1. Spatial Expression of *RsMYB1* and *RsTT8* Affects Anthocyanin Accumulation in Radish Taproot

The tissue-specific expression of genes encoding MYB or bHLH TFs has been shown to control the site and timing of anthocyanin biosynthesis [32,33]. We confirmed that *RsMYB1* and *RsTT8* transcript levels correlated well with the extent of anthocyanin accumulation in the skin and flesh of taproots, as well as with transcript levels of early (EBG) and late (LBG) anthocyanin biosynthetic genes (Figure 2).

Importantly, we found that radish cultivars with white taproots produce *RsMYB1* transcripts that are predicted to encode a shorter protein, *RsMYB1<sup>Short</sup>*, with the 4 bp insertion in the first exon, causing a premature stop codon that terminates the protein at only about one-fifth of its functional length (Figure 3 and Supplementary Figure S1). We identified this insertion only in radish cultivars with white taproots, but not in those with red taproots, although some white-taproot cultivars were heterozygous for the *RsMYB1<sup>Short</sup>* and *RsMYB1<sup>Full</sup>* alleles (Figure 10).

In view of previous studies reporting that anthocyanin biosynthesis requires the interaction of *RsMYB1* and *RsTT8* [12], we investigated the molecular consequences of *RsMYB1<sup>Short</sup>* on protein–protein interactions, and found that *RsTT8* interacted with only *RsMYB1<sup>Full</sup>*, not *RsMYB1<sup>Short</sup>*. We also refined the interaction interface between *RsMYB1* and *RsTT8*, showing the R3 domain of *RsMYB1* was an indispensable region with the MIR at the N terminus of *RsTT8*. Indeed, the truncated version of *RsMYB1*, *RsMYB1<sup>Short</sup>*, lacking the R3 domain failed to interact with either full-length or partially truncated versions of its cognate partner, *RsTT8*. We confirmed that *RsMYB1<sup>Short</sup>* was unable to transactivate the *RsCHS* and *RsDFR* promoters and did not result in anthocyanin accumulation when transiently overexpressed in radish cotyledons or tobacco leaves, expected by the loss of ability to interact with *RsTT8*. These results demonstrate that the interaction of *RsMYB1* and *RsTT8* can transcriptionally activate the anthocyanin biosynthetic genes and lead to anthocyanin accumulation.

### 3.2. The Allelic Variant *RsMYB1<sup>Short</sup>* Lack of Function in Anthocyanin Biosynthesis

R2R3 MYB TFs have a highly conserved DNA-binding domain at their N terminus and a highly variable region at their C terminus, harboring the activation or repression motif that contributes to their functional grouping [34]. At the N terminus, each R2 and R3 domain consists of an imperfect repeat (R) of about 52 amino acids in length and forms three  $\alpha$ -helices, resulting in a helix-turn-helix protein architecture that conforms to the major groove of genomic DNA [30]. Several studies reported that the R2 and R3 domains play an important role in the recognition of the DNA backbone, as well as the interaction with counterpart bHLH TFs. For example, in white-flowered lily (*Lilium speciosum*), a single amino acid substitution at a conserved aromatic residue (Trp to Leu) in the R2 repeat of the R2R3 MYB TF *LsMYB12* completely suppresses anthocyanin biosynthesis [35]. Additionally, the transcript levels of *LsMYB12<sup>WtoL</sup>* are very low and lead to reduced transcription of anthocyanin biosynthetic genes, resulting in the absence of pigmentation in tepals. In tomato *SIAN2like<sup>WT</sup>*, alternative splicing of R2R3 MYB *SIAN2-like* led to the formation of the dysfunctional protein with only an R2 domain, which showed the complete loss of anthocyanin accumulation in fruit peel [21]. Additionally, *SIAN2like<sup>WT</sup>* lost the ability to interact with bHLH partners, indicating that the formation of the MBW complex was not affected.

We demonstrated here that the *RsMYB1<sup>Short</sup>* transcripts encode truncated proteins with the loss of most of the downstream residue of the R2 domain. The R3 domain of R2R3 MYB TFs, orchestrating anthocyanin accumulation, is important for their interaction with the MIR of flavonoid-related bHLH TFs. This interaction is a prerequisite for the assembly of the anthocyanin-activating MBW complex [34]. The protein encoded by the allelic variant *RsMYB1<sup>Short</sup>* exhibited abnormal subcellular distribution and lost the ability to physically interact with *RsTT8* (Figures 4 and 5). As expected, the simultaneous transient co-overexpression of *RsMYB1<sup>Short</sup>* and *RsTT8* did not activate the transcription of anthocyanin biosynthetic genes or result in anthocyanin accumulation. These results suggest that *RsMYB1<sup>Short</sup>*, a truncated protein with a partial R2 domain, should abolish the transcriptional regulation of anthocyanin biosynthetic genes and interfere with the formation of the MBW complex.

Another possible explanation is that the aberrant *RsMYB1<sup>Short</sup>* might affect the transcript levels of *RsTT8*, thus decreasing *RsTT8* accumulation and interfering with formation of the MBW complex. Although the *RsTT8* locus in the white and red cultivars encoded the



same protein, *RsTT8* transcript levels were very low in the taproot of the white cultivars tested here. Indeed, many studies have shown that R2R3 MYB enhances the transcription of the genes encoding the bHLH component of the MBW complex [36–38]. The Arabidopsis R2R3 MYB TFs' production of anthocyanin pigment 1 (AtPAP1) and AtTT2 and tomato *SIAN4* can increase the transcription of the bHLH-encoding genes *AtTT8* and *SIAN1*, respectively [36,38]. Taken together, these results suggest that the dysfunctional R2R3 MYB proteins interfere with the conformation of the active MBW complex by reducing the transcription of bHLH TF-encoding genes.

Self-regulation of *RsMYB1* by RsMYB1 may also contribute to the lack of anthocyanin biosynthesis in white radishes. Previous studies reported that the transcription of *Md-MYB10* in red-fleshed apples is self-regulated by MdMYB10 binding to its promoter [22]. As RsMYB1<sup>Short</sup> only harbors a partial R2 domain, we hypothesize that RsMYB1<sup>Short</sup> may no longer be able to activate the expression of its own encoding gene, which would contribute to the loss of anthocyanin accumulation in white cultivars.

Taken together, our results demonstrate that RsMYB1 was crucial for the accumulation of anthocyanins in radish taproots. However, genotyping of multiple cultivars with the CAPS marker developed in this study also revealed that several radish cultivars with white taproots are heterozygous for the *RsMYB1*<sup>Short</sup> allele. This observation indicates that polymorphisms in other structural and/or regulatory genes contribute to taproot coloration in addition to *RsMYB1*, which is an area for future research. Based on these results, the color of radish roots can be engineered through knowledge-based molecular marker development or manipulation of key genes via genome editing.

## 4. Materials and Methods

### 4.1. Plant Materials

Radish plants were grown in the field under short-day conditions at the National Institute of Agricultural Sciences (Jeonju, Korea). The following six radish cultivars with different root skin colors were used in this study and will be referred to as W1–W3 (for radishes with white taproots) and R1–R3 (for radishes with red taproots): W1, '939' (from Asia seed Co., Seoul, Korea); W2, 'BaePi' (from Nongwoo seed Co., Suwon, Korea); W3, '948' (Asia); R1, 'HongPi' (Nongwoo); R2, '890' (Asia); and R3, 'BoraKing' (Asia). Anthocyanin and the transcript levels of anthocyanin-related genes were analyzed in root skins and root flesh.

For cleaved amplified polymorphic sequences (CAPS) marker analysis, we used a set of 20 radish germplasm obtained from the Agricultural Genetic Resources Center at the National Institute of Agricultural Science (Jeonju, Korea) and from seed companies: the white radishes 'IT100606', 'IT100613', 'IT100615', '939', 'IT250795', 'IT276165', BaePi, 948 (Asia) and '60471' (Asia); and the red/purple radishes 'IT261944', 'IT2619478', 'IT262050', 'IT308359', HongPi, 890, BoraKing, 'Artesia' (Asia), and '6217' (Asia).

Transient expression assays with radish cotyledons were conducted using plants of the commercial F<sub>1</sub> hybrid cultivar 'DanHong' (Asia Seed Co.), which were grown in a growth chamber under long day conditions (16 h light/8 h dark) at 22 °C. Tobacco (*Nicotiana tabacum*) plants grown in greenhouses under natural light at 28 °C were used for transient *Agrobacterium* (*Agrobacterium tumefaciens*)-mediated infiltration assays. All samples were frozen rapidly in liquid nitrogen and stored at –80 °C. A portion of each sample was then used for RNA extraction and anthocyanin measurements.

### 4.2. RNA Extraction, cDNA Synthesis, and Genomic DNA Isolation

Total RNA was extracted from 100 mg of taproots of radish cultivars using the Fruit-mate for RNA Purification solution (Takara, Otsu, Japan) for removal of polysaccharides and polyphenols and Plant RNA Purification Reagent (Invitrogen, Carlsbad, CA, USA) as described previously [39] and purified using the FavorPrep Plant Total RNA Mini Kit (Favorgen, Changzhi, Taiwan). Total RNA was prepared from 100 mg of tobacco leaves using TRIzol reagent (Invitrogen) and purified using the FavorPrep Plant Total RNA Mini

Kit (Favorgen), according to the manufacturer's instructions. DNA contamination was removed by DNase I digestion (Ambion, Thermo Fisher Scientific, MA, USA). First-strand cDNA was synthesized from 2 µg of total RNA using the amfiRivert cDNA Synthesis Platinum Master Mix (GenDEPOT, Barker, TX, USA).

Genomic DNA was extracted from 100 mg of radish leaves using the Plant Mini Kit (Qiagen, Valencia, CA, USA) according to the manufacturer's instructions.

#### 4.3. Measurement of Total Anthocyanin Contents

Total anthocyanin contents in root skins and root flesh were determined according to the method described by [39]. Briefly, samples were ground to powder in liquid nitrogen. Aliquots of 100 mg fresh weight were then mixed in 600 µL extraction buffer (methanol containing 1% (v/v) HCl) for 6 h at 4 °C with moderate agitation. An addition of 200 µL water and 200 µL chloroform was followed by centrifugation to pellet plant debris at 14,000× *g* for 5 min at 4 °C. After centrifugation, absorbance of the supernatant was recorded at 530 nm ( $A_{530}$ ) and 657 nm ( $A_{657}$ ) using a microplate reader. Anthocyanin content was determined according to the formula  $A_{530} - (0.33 \times A_{657})$ . Each sample was extracted and measured from three independent experiments.

#### 4.4. RT-qPCR Analysis

Transcript levels were determined by RT-qPCR using the AccuPower 2x Greenstar qPCR Master Mix (Bioneer, Daejeon, Korea) and the Bio-Rad CFX96 Detection System (Bio-Rad Laboratories, Hercules, CA, USA) according to the manufacturer's instructions. The RT-qPCR conditions were used as follows: pre-denaturation at 95 °C for 5 min, 40 cycles of denaturation at 95 °C for 15 s, and annealing at 55 °C for 30 s. Gene expression was normalized using *RNA POLYMERASE II (RPII)* and *GLYCERALDEHYDE 3-PHOSPHATE DEHYDROGENASE (GAPDH)* for radish and tobacco, respectively, as the reference gene. Three independent biological replicates were performed per sample. The primers used for RT-qPCR analysis are listed in Supplementary Table S1.

#### 4.5. Gene Cloning and Sequence Analysis

The full-length open reading frames (ORFs) of *RsMYB1* were amplified from cDNA and genomic DNA derived from white radish (W1) and red radish (R1) cultivars by PCR with PrimeSTAR HS DNA Polymerase (Takara, Japan) using the primer pair *RsMYB1 F/R* (Supplementary Table S1). The PCR conditions were used as follows: pre-denaturation at 98 °C for 5 min, followed by 35 at 98 °C for 20 s, at 56 °C for 20 s, and at 72 °C for 60 s, and final extension at 72 °C for 5 min. All PCR amplicons were subcloned into the pENTR/D-TOPO vector (Invitrogen) for validation sequencing.

The nucleotide sequences, deduced protein sequences, and ORFs of *RsMYB1* from the W1 and R1 cultivars were analyzed online (<http://www.ncbi.nlm.nih.gov>, accessed on 13 September 2021). Structural analysis of the deduced proteins was carried out at the ExPASy Molecular Biology Server (<http://cn.expasy.org/tools/>, accessed on 13 September 2021). Multiple sequence alignments were generated using the CLUSTALW program (<https://www.genome.jp/tools-bin/clustalw>, accessed on 13 September 2021). A phylogenetic tree was constructed using the neighbor-joining method [40] with MEGA version 6 software [41].

#### 4.6. Subcellular Localization Assay

The subcellular localization of *RsMYB1<sup>Short</sup>* and *RsMYB1<sup>Full</sup>* was analyzed in *Arabidopsis* protoplasts as described by [42]. Green fluorescent protein (GFP) fusion constructs were generated in the p326-sGFP plasmid, which contains the Cauliflower mosaic virus (CaMV) 35S promoter. For C-terminal GFP fusions, the ORFs of *RsMYB1<sup>Short</sup>* and *RsMYB1<sup>Full</sup>* were individually amplified using gene-specific primer sets (p326-*RsMYB1<sup>Short</sup>*-F/R and p326-*RsMYB1<sup>Full</sup>*-F/R), which introduced an *XbaI* restriction site upstream of the ATG codon, using the InFusion Cloning System (Clontech). The resulting p326-

RsMYB1<sup>Short</sup>-sGFP and p326-RsMYB1<sup>Full</sup>-sGFP were sequenced to confirm the absence of errors during PCR amplification. The plasmids were introduced into *Arabidopsis* mesophyll protoplasts by polyethylene-glycol-mediated transformation. After incubation for 16–20 h at 25 °C in the dark, images were captured by fluorescence confocal microscopy (Leica TCS SP8, Leica Microsystems, Germany).

#### 4.7. Transactivation and Yeast Two-Hybrid (Y2H) Assays

To generate the RsMYB1<sup>Short</sup>, RsMYB1<sup>Full</sup>, and RsTT8 constructs, full-length or truncated versions of the RsMYB1<sup>Full</sup> and RsTT8 ORFs were individually amplified using specific primer sets (Supplementary Table S1). The amplified fragments RsMYB1<sup>Short</sup> and RsMYB1<sup>Full</sup> were then cloned in-frame with the sequence encoding the GAL4 DNA-binding domain (BD) into pGBKT7 using the In-Fusion Cloning System (Clontech). Similarly, full-length or truncated versions of the RsTT8 coding sequence were individually cloned in-frame with the sequence of the GAL4 activation domain (AD) into pGADT7. The AD and BD constructs were co-transformed into yeast (*Saccharomyces cerevisiae*) strain MaV203 following the manufacturer's instructions (Takara). Yeast colonies were selected on synthetic defined (SD) medium lacking Trp and Leu and were replicated on SD medium lacking Trp, Leu, and His containing 10 mM 3-amino-1,2,4-triazole (3-AT), a competitive inhibitor of the *HIS3* gene product. The plates were photographed after 2 d of incubation in the dark at 30 °C.

#### 4.8. In Planta Assays of RsMYB1 Function

The plasmid used in tobacco and radish transient expression assays was constructed as follows. The genomic and cDNA sequences of RsMYB1<sup>Short</sup> and RsMYB1<sup>Full</sup> were amplified with specific primer sets (Supplementary Table S1), and cloned into the pENTR/D-TOPO vector (Invitrogen). For transient assays, the above cloned RsMYB1<sup>Short</sup> and RsMYB1<sup>Full</sup> PCR amplicons were incorporated into the Gateway destination vector pB7WG2D (VIB-Ghent University, Ghent, Belgium) through several Gateway cloning steps. The resulting vectors were introduced into *Agrobacterium* strain GV3101 for transient infiltration of the abaxial leaf surface of radish (*Raphanus sativus* cv. 'DanHong') and tobacco (*Nicotiana tabacum* cv. Xanthi) plants. Leaf color was monitored 5 d later as described in [27].

#### 4.9. Promoter Activation Assay

The RsCHS and RsDFR promoter regions were individually PCR amplified and then cloned into the pTr-GUS vector to generate reporter constructs as previously described [12]. The ORFs of RsMYB1<sup>Short</sup>, RsMYB1<sup>Full</sup>, and RsTT8 were individually subcloned into the pENTR/D-TOPO vector (Invitrogen) and incorporated into the Gateway destination vector pB2GW7 (VIB-Ghent University, Ghent, Belgium) using several Gateway cloning steps. The resulting constructs pB2GW7-RsMYB1<sup>Short</sup>, pB2GW7-RsMYB1<sup>Full</sup>, and pB2GW7-RsTT8 were used as effector constructs. All constructs were transformed into *Agrobacterium* strain GV3101.

Transient promoter activation assays were performed in tobacco as previously described [12]. Briefly, *Agrobacterium* containing individual reporter or effector constructs were grown in LB medium for 2 d at 28 °C, pelleted by centrifugation at 3500× *g* for 5 min at 4 °C, resuspended in infiltration buffer (10 mM MgCl<sub>2</sub> and 100 μM acetosyringone) to an OD<sub>600</sub> of 0.2 (approximately 10 mL of buffer), and incubated at room temperature without shaking for 2 h. Prior to infiltration into tobacco leaves, *Agrobacterium* harboring effector and reporter constructs were mixed in a 1:3 ratio. Tobacco leaves were infiltrated with *Agrobacterium* harboring the genes of interest and harvested to assay GUS activity 3 d later. *Agrobacterium* harboring only the *GUS* reporter construct were used as controls. At least three independent biological replicates were performed for each experiment.

#### 4.10. Molecular Marker for Discrimination of Radish Skin Color

Radish genomic DNA from 20 cultivars (10 white and 10 red/purple) was used to test markers that would discriminate cultivars based on taproot color. PCR was performed with a primer pair for the cleaved amplified polymorphic sequence (CAPS) marker designed against *RsMYB1*. The PCR conditions were as follows: denaturation at 98 °C for 2 min, followed by 30 cycles of 98 °C for 10 s, 60 °C for 15 s, and 68 °C for 30 s. For CAPS analysis, PCR amplicons were digested with *Mlu*CI, separated on a 1.5% agarose gel, and visualized by staining with ethidium bromide.

## 5. Conclusions

In this study, we demonstrated that anthocyanin biosynthesis is determined in part by allelic variation at the *RsMYB1* locus in the form of the *RsMYB1<sup>Short</sup>* and *RsMYB1<sup>Full</sup>* alleles. Sequence analysis revealed a 4 bp insertion in the white allele *RsMYB1<sup>Short</sup>* in the first exon, leading to a frameshift mutation that produced the truncated protein with a partial R2 domain. In radish cultivars with red taproots, anthocyanin accumulation and anthocyanin biosynthetic gene expression strongly depended on the transcript levels of *RsMYB1<sup>Full</sup>* and *RsTT8*. A transient expression assay with radish cotyledons indicated that *RsMYB1<sup>Short</sup>* may encode a non-functional protein that fails to induce the accumulation of anthocyanins. Promoter activation assays and transient expression assays in tobacco demonstrated that co-expressing *RsMYB1<sup>Full</sup>* and *RsTT8* activated anthocyanin accumulation and *RsCHS* and *RsDFR* transcription, whereas co-expressing *RsMYB1<sup>Short</sup>* and *RsTT8* did not. Taken together, these results suggest that the *RsMYB1* allele plays a key role in shaping anthocyanin accumulation in the radish taproot.

**Supplementary Materials:** The following are available online at <https://www.mdpi.com/article/10.3390/ijms222010927/s1>. Figure S1: Multiple alignment of the genomic sequence of *RsMYB1* derived from red (*RsMYB1<sup>Full</sup>*) and white (*RsMYB1<sup>Short</sup>*) radish and the previously reported *RsMYB1* genomic sequence from the Bordeaux cultivar, Figure S2: Phylogenetic relationships between anthocyanin biosynthetic regulators in radish and other species, Table S1: List of primers used in this study.

**Author Contributions:** S.-H.L. and J.-Y.L. conceived and designed the research and drafted the manuscript. D.-H.K. conducted molecular biology experiments. J.L. and J.R. cultivated the radishes in the field. All authors contributed to the article and approved the submitted version. All authors have read and agreed to the published version of the manuscript.

**Funding:** This research was funded by grants from the BioGreen21 Agri-Tech Innovation Program (PJ015734), the Cooperative Research Program for Agriculture Science and Technology Development (PJ014554), the Rural Development Administration, and from the Basic Science Research Program through the National Research Foundation of Korea (NRF-2020R1F1A1072559), the Ministry of Education, Korea.

**Institutional Review Board Statement:** Not applicable.

**Informed Consent Statement:** Not applicable.

**Data Availability Statement:** Not applicable.

**Conflicts of Interest:** The authors declare that the research was conducted in the absence of any commercial or financial relationships that could be construed as a potential conflict of interest.

## References

1. Harborne, J.; Williams, C. Advances in flavonoid research since 1992. *Phytochemistry* **2000**, *55*, 481–504. [[CrossRef](#)]
2. Nakabayashi, R.; Yonekura-Sakakibara, K.; Urano, K.; Suzuki, M.; Yamada, Y.; Nishizawa, T.; Matsuda, F.; Kojima, M.; Sakakibara, H.; Shinozaki, K.; et al. Enhancement of oxidative and drought tolerance in *Arabidopsis* by overaccumulation of antioxidant flavonoids. *Plant J.* **2014**, *77*, 367–379. [[CrossRef](#)] [[PubMed](#)]
3. Ross, J.A.; Kasum, C.M. Dietary flavonoids: Bioavailability, metabolic effects, and safety. *Annu. Rev. Nutr.* **2002**, *22*, 19–34. [[CrossRef](#)]
4. Zhang, Y.; Butelli, E.; Martin, C. Engineering anthocyanin biosynthesis in plants. *Curr. Opin. Plant Biol.* **2014**, *19*, 81–90. [[CrossRef](#)]



5. Vinayagam, R.; Xu, B. Antidiabetic properties of dietary flavonoids: A cellular mechanism review. *Nutr. Metab.* **2015**, *12*, 1–20. [[CrossRef](#)]
6. Winkel-Shirley, B. Flavonoid biosynthesis. A colorful model for genetics, biochemistry, cell biology, and biotechnology. *Plant Physiol.* **2001**, *126*, 485–493. [[CrossRef](#)] [[PubMed](#)]
7. Hichri, I.; Barrieu, F.; Bogs, J.; Kappel, C.; Delrot, S.; Lauvergeat, V. Recent advances in the transcriptional regulation of the flavonoid biosynthetic pathway. *J. Exp. Bot.* **2011**, *62*, 2465–2483. [[CrossRef](#)] [[PubMed](#)]
8. Petroni, K.; Tonelli, C. Recent advances on the regulation of anthocyanin synthesis in reproductive organs. *Plant Sci.* **2011**, *181*, 219–229. [[CrossRef](#)]
9. Nesi, N.; Jond, C.; Debeaujon, I.; Caboche, M.; Lepiniec, L. The Arabidopsis *TT2* gene encodes an R2R3 MYB domain protein that acts as a key determinant for proanthocyanidin accumulation in developing seed. *Plant Cell* **2001**, *13*, 2099–2114. [[CrossRef](#)]
10. Liu, Y.; Lin-Wang, K.; Espley, R.V.; Wang, L.; Yang, H.; Yu, B.; Dare, A.; Varkonyi-Gasic, E.; Wang, J.; Zhang, J.; et al. Functional diversification of the potato R2R3 MYB anthocyanin activators AN1, MYBA1, and MYB113 and their interaction with basic helix-loop-helix cofactors. *J. Exp. Bot.* **2016**, *67*, 2159–2176. [[CrossRef](#)]
11. Xu, W.; Dubos, C.; Lepiniec, L. Transcriptional control of flavonoid biosynthesis by MYB-bHLH-WDR complexes. *Trends Plant Sci.* **2015**, *20*, 176–185. [[CrossRef](#)] [[PubMed](#)]
12. Lim, S.H.; Kim, D.H.; Kim, J.K.; Lee, J.Y.; Ha, S.H. A radish basic helix-loop-helix transcription factor, RsTT8 acts a positive regulator for anthocyanin biosynthesis. *Front Plant Sci.* **2017**, *8*, 1917. [[CrossRef](#)] [[PubMed](#)]
13. Ramsay, N.A.; Glover, B.J. MYB-bHLH-WD40 protein complex and the evolution of cellular diversity. *Trends Plant Sci.* **2005**, *10*, 63–70. [[CrossRef](#)]
14. Gonzalez, A.; Zhao, M.; Leavitt, J.M.; Lloyd, A.M. Regulation of the anthocyanin biosynthetic pathway by the TTG1/bHLH/Myb transcriptional complex in Arabidopsis seedlings. *Plant J.* **2008**, *53*, 814–827. [[CrossRef](#)] [[PubMed](#)]
15. Kiferle, C.; Fantini, E.; Bassolino, L.; Povero, G.; Spelt, C.; Buti, S.; Giuliano, G.; Quattrocchio, F.; Koes, R.; Perata, P.; et al. Tomato R2R3-MYB proteins SLANT1 and SLANT2: Same protein activity, different roles. *PLoS ONE* **2015**, *10*, e0136365. [[CrossRef](#)] [[PubMed](#)]
16. Albert, N.W.; Davies, K.M.; Lewis, D.H.; Zhang, H.; Montefiori, M.; Brendolise, C.; Boase, M.R.; Ngo, H.; Jameson, P.E.; Schwinn, K.E.; et al. A conserved network of transcriptional activators and repressors regulates anthocyanin pigmentation in eudicots. *Plant Cell* **2014**, *26*, 962–980. [[CrossRef](#)] [[PubMed](#)]
17. Costantini, L.; Malacarne, G.; Lorenzi, S.; Troggio, M.; Mattivi, F.; Moser, C.; Grando, M.S. New candidate genes for the fine regulation of the colour of grapes. *J. Exp. Bot.* **2015**, *66*, 4427–4440. [[CrossRef](#)]
18. Huang, D.; Wang, X.; Tang, Z.; Yuan, Y.; Xu, Y.; He, J.; Jiang, X.; Peng, S.A.; Li, L.; Butelli, E.; et al. Subfunctionalization of the *Ruby2-Ruby1* gene cluster during the domestication of citrus. *Nat. Plants* **2018**, *4*, 930–941. [[CrossRef](#)]
19. Castillejo, C.; Waurich, V.; Wagner, H.; Ramos, R.; Oiza, N.; Muñoz, P.; Triviño, J.C.; Caruana, J.; Liu, Z.; Cobo, N.; et al. Allelic Variation of *MYB10* Is the Major Force Controlling Natural Variation in Skin and Flesh Color in Strawberry (*Fragaria* spp.) Fruit. *Plant Cell* **2020**, *32*, 3723–3749. [[CrossRef](#)]
20. He, Q.; Wu, J.; Xue, Y.; Zhao, W.; Li, R.; Zhang, L. The novel gene *BrMYB2*, located on chromosome A07, with a short intron 1 controls the purple-head trait of Chinese cabbage (*Brassica rapa* L.). *Hortic. Res.* **2020**, *7*, 1–19. [[CrossRef](#)]
21. Colanero, S.; Tagliani, A.; Perata, P.; Gonzali, S. Alternative splicing in the *anthocyanin fruit* gene encoding an R2R3 MYB transcription factor affects anthocyanin biosynthesis in tomato fruits. *Plant Commun.* **2020**, *1*, 100006. [[CrossRef](#)]
22. Espley, R.V.; Brendolise, C.; Chagne, D.; Kuttly-Amma, S.; Green, S.; Volz, R.; Putterill, J.; Schouten, H.J.; Gardiner, S.E.; Hellens, R.P.; et al. Multiple repeats of a promoter segment causes transcription factor autoregulation in red apples. *Plant Cell* **2009**, *21*, 168–183. [[CrossRef](#)]
23. Butelli, E.; Licciardello, C.; Zhang, Y.; Liu, J.; Mackay, S.; Bailey, P.; Reforgiato-Recupero, G.; Martin, C. Retrotransposons control fruit-specific, cold-dependent accumulation of anthocyanins in blood oranges. *Plant Cell* **2012**, *24*, 1242–1255. [[CrossRef](#)]
24. Jung, S.; Venkatesh, J.; Kang, M.Y.; Kwon, J.K.; Kang, B.C. A non-LTR retrotransposon activates anthocyanin biosynthesis by regulating a MYB transcription factor in *Capsicum annuum*. *Plant Sci.* **2019**, *287*, 110181. [[CrossRef](#)]
25. Park, N.I.; Xu, H.; Li, X.; Jang, I.H.; Park, S.; Ahn, G.H.; Lim, Y.P.; Kim, S.J.; Park, S.U. Anthocyanin accumulation and expression of anthocyanin biosynthetic genes in radish (*Raphanus sativus*). *J. Agric. Food Chem.* **2011**, *59*, 6034–6039. [[CrossRef](#)] [[PubMed](#)]
26. Chen, F.; Xing, C.; Huo, S.; Cao, C.; Yao, Q.; Fang, P. Red pigment content and expression of genes related to anthocyanin biosynthesis in radishes (*Raphanus sativus* L.) with different colored flesh. *J. Agric. Sci.* **2016**, *8*, 126–135. [[CrossRef](#)]
27. Lim, S.H.; Song, J.H.; Kim, D.H.; Kim, J.K.; Lee, J.Y.; Kim, Y.M.; Ha, S.H. Activation of anthocyanin biosynthesis by expression of the radish R2R3-MYB transcription factor gene *RsMYB1*. *Plant Cell Rep.* **2016**, *35*, 641–653. [[CrossRef](#)]
28. Yi, G.; Kim, J.S.; Park, J.E.; Shin, H.; Yu, S.H.; Park, S.; Huh, J.H. MYB1 transcription factor is a candidate responsible for red root skin in radish (*Raphanus sativus* L.). *PLoS ONE* **2018**, *13*, e0204241. [[CrossRef](#)] [[PubMed](#)]
29. Luo, X.B.; Xu, L.; Wang, Y.; Dong, J.H.; Chen, Y.L.; Tang, M.J.; Fan, L.; Zhu, Y.; Liu, L. An ultra-high density genetic map provides insights into genome synteny, recombination landscape and taproot skin color in radish (*Raphanus sativus* L.). *Plant Biotechnol. J.* **2020**, *18*, 274–286. [[CrossRef](#)]
30. Wang, Q.; Wang, Y.; Sun, H.; Sun, L.; Zhang, L. Transposon-induced methylation of the *RsMYB1* promoter disturbs anthocyanin accumulation in red-fleshed radish. *J. Exp. Bot.* **2020**, *71*, 2537–2550. [[CrossRef](#)] [[PubMed](#)]



31. Masukawa, T.; Cheon, K.S.; Mizuta, D.; Nakatsuka, A.; Kobayashi, N. Insertion of a retrotransposon into a *flavonoid 3'-hydroxylase* homolog confers the red root character in the radish (*Raphanus sativus* L. var. *longipinnatus* L. H. Bailey). *Hort. J.* **2018**, *87*, 89–96. [[CrossRef](#)]
32. Yamagishi, M.; Shimoyamada, Y.; Nakatsuka, T.; Masuda, K. Two *R2R3-MYB* genes, homologs of petunia *AN2*, regulate anthocyanin biosyntheses in flower tepals, tepal spots and leaves of Asiatic hybrid lily. *Plant Cell Physiol.* **2010**, *51*, 463–474. [[CrossRef](#)]
33. Yuan, Y.W.; Sagawa, J.M.; Frost, L.; Vela, J.P.; Bradshaw, H.D., Jr. Transcriptional control of floral anthocyanin pigmentation in monkeyflowers (*Mimulus*). *New Phytol.* **2014**, *204*, 1013–1027. [[CrossRef](#)]
34. Millard, P.S.; Kragelund, B.B.; Burow, M. R2R3 MYB transcription factors-Functions outside the DNA-binding domain. *Trends Plant Sci.* **2019**, *24*, 934–946. [[CrossRef](#)]
35. Suzuki, K.; Tasaki, K.; Yamagishi, M. Two distinct spontaneous mutations involved in white flower development in *Lilium speciosum*. *Mol. Breeding* **2015**, *35*, 1–14. [[CrossRef](#)]
36. Baudry, A.; Caboche, M.; Lepiniec, L. TT8 controls its own expression in a feedback regulation involving TTG1 and homologous MYB and bHLH factors, allowing a strong and cell-specific accumulation of flavonoids in *Arabidopsis thaliana*. *Plant J.* **2006**, *46*, 768–779. [[CrossRef](#)]
37. Montefiori, M.; Brendolise, C.; Dare, A.P.; Lin-Wang, K.; Davies, K.M.; Hellens, R.P.; Allan, A.C. In the Solanaceae, a hierarchy of bHLHs confer distinct target specificity to the anthocyanin regulatory complex. *J. Exp. Bot.* **2015**, *66*, 1427–1436. [[CrossRef](#)]
38. Spelt, C.; Quattrocchio, F.; Mol, J.N.; Koes, R. *anthocyanin1* of petunia encodes a basic helix-loop-helix protein that directly activates transcription of structural anthocyanin genes. *Plant Cell* **2000**, *12*, 1619–1631. [[CrossRef](#)]
39. Lim, S.H.; Park, B.; Kim, D.H.; Park, S.; Yang, J.H.; Jung, J.A.; Lee, J.; Lee, J.Y. Cloning and functional characterization of dihydroflavonol 4-reductase gene involved in anthocyanin biosynthesis of Chrysanthemum. *Int. J. Mol. Sci.* **2020**, *21*, 7960. [[CrossRef](#)]
40. Saitou, N.; Nei, M. The neighbor-joining method: A new method for reconstructing phylogenetic trees. *Mol. Biol. Evol.* **1987**, *4*, 406–425.
41. Kumar, S.; Tamura, K.; Jakobsen, I.B.; Nei, M. MEGA2: Molecular evolutionary genetics analysis software. *Bioinformatics* **2001**, *17*, 1244–1245. [[CrossRef](#)]
42. Yoo, S.D.; Cho, Y.H.; Sheen, J. Arabidopsis mesophyll protoplasts: A versatile cell system for transient gene expression analysis. *Nat. Protoc.* **2007**, *2*, 1565–1572. [[CrossRef](#)]